Extension of the relationship to larger clusters is obvious, demonstrating the expansion (41).

It is easily seen that any term in (A6) corresponding to a choice of integers $\{P_{ij}\}$ vanishes if the nonzero integers P_{ij} can be divided into two sets with no indices in common. That is, all "unlinked diagrams" vanish. This follows from the fact that, in generating the term by operating with the D's we can first apply all the D_{kl} in one set. When we then apply a D_{ij} from the second (nonoverlapping) set, the quantity immediately vanishes. To see this we let $\langle \phi \rangle$ be one of the averages generated by the D_{kl} of the first set so that ϕ involves

only the $\mathcal{K}_{kl}$ in this set. We can let all the γ_{ki} which join the two sets vanish, and ρ_γ factors into $\rho_1\rho_2$ where ρ_1 involves the spins of the first set and ρ_2 involves the spins of the second set. Then

$$\langle \phi \rangle = \mathrm{tr}\phi\rho_1\rho_2/\mathrm{tr}\rho_1\rho_2 = (\mathrm{tr}\phi\rho_1)(\mathrm{tr}\rho_2)/(\mathrm{tr}\rho_1)(\mathrm{tr}\rho_2)$$
$$= \mathrm{tr}(\phi\rho_1)/\mathrm{tr}\rho_1, \quad \text{(A11)}$$

and this quantity is independent of the indices of the second set. Hence, if D_{ij} belongs in the second set, $D_{ij}\langle \phi \rangle = 0$, proving that all such unlinked diagrams vanish.

Critical Fields of Thin Superconducting Films. II. Mean Free Path Effects in Indium-Tin Alloy Films

A. M. Toxen and M. J. Burns

Thomas J. Watson Research Center, International Business Machines Corporation, Yorktown Heights, New York

(Received 5 October 1962; revised manuscript received 25 February 1963)

In a previous paper, a theoretical model was presented from which the critical magnetic fields of thin superconducting films could be calculated. The model was worked out for the nonlocal model of Pippard, but only thickness effects were discussed in detail and compared to experimental data on pure indium films. In this paper, mean free path effects as well as thickness effects are discussed, and the results are found to be in good agreement with critical field measurements on thin alloy films of indium containing 0–4.6 at.% tin, if one assumes that $\xi_0\lambda_L{}^2$ is equal to 1.62×10^9 (Å)^3 at $0.9T_c$, ξ_0 is equal to 2600 Å, and ρl is approximately 2.0×10^{-11} Ω-cm^2. For these values of ξ_0 and ρl, the coherence length, ξ, has been calculated for each film from measurements of resistivity and thickness, and is found to vary from 2600 Å at 0 at.% Sn to 1000 Å at 4.6 at.% Sn. Also, the question of whether size effects in thin films are equivalent to mean free path effects is discussed in detail. It is concluded that size effects are not equivalent to mean free path effects, or more precisely, boundary scattering is not equivalent to scattering by randomly distributed defects. In fact, it is demonstrated that whereas the London or "local" limit obtains in the presence of high concentrations of randomly distributed defects, the Pippard or "nonlocal" limit obtains in very thin films, where boundary scattering predominates.

1. INTRODUCTION

IN a previous paper,[1] hereafter referred to as I, a theoretical model was presented which relates the critical magnetic fields of thin superconducting films to the kernel of the current-vector-potential relationship for any theory of superconductivity. The model was worked out for the nonlocal theory of Pippard,[2] but only thickness effects were discussed in detail and compared to experimental data. In this paper, mean free path effects, as well as thickness effects, will be discussed and compared to critical field data obtained for indium-tin alloy films. The theoretical discussion will be limited to the nonlocal theory of Pippard with specular boundary conditions. Because of the similarity between the kernels of the Pippard and BCS[3] theories, it is expected that the results are substantially the same that would be obtained from the BCS kernel. In addition, the ques-

tion of whether size effects in thin films are equivalent to mean free path effects is discussed in detail.

2. THEORETICAL

For the case of the Pippard kernel with specular boundary conditions, an expression for the critical field is derived in I which is of the form

$$h_c/H_c = g(\xi_0\lambda_L{}^2/a^3, \xi/a), \quad \text{(1)}$$

where h_c is the critical field of the film, H_c is the bulk critical field, ξ is the coherence distance, ξ_0 is the coherence distance in pure material, λ_L is the London penetration depth, a is the half-thickness of the film, and g is a function which can be numerically evaluated. The evaluation is carried out most conveniently in two steps. First, the film susceptibility is calculated from the results of Schrieffer,[4]

$$\left(\frac{\kappa}{\kappa_0}\right)_{\mathrm{spec}} = 1 - \frac{2}{a^2}\sum_{n=0}^{\infty}[k_n{}^2 + K(k_n)]^{-1}, \quad \text{(2)}$$

[1] A. M. Toxen, Phys. Rev. 127, 382 (1962).
[2] A. B. Pippard, Proc. Roy. Soc. (London) A216, 547 (1953).
[3] J. Bardeen, L. N. Cooper, and J. R. Schrieffer, Phys. Rev. 108, 1175 (1957).
[4] J. R. Schrieffer, Phys. Rev. 106, 47 (1957).

where $k_n = (2n+1)\pi/2a$, and $K(k_n)$ is the kernel obtained from the relationship between the supercurrent density and the vector potential in wave vector space. The quantities κ and κ_0 are, respectively, the film and bulk susceptibilities in a weak magnetic field. The kernel, $K(k)$, is defined by the relationship

$$(-4\pi/c)\mathbf{j}(k) \equiv K(k)\mathbf{A}(k),\qquad (3)$$

where $\mathbf{j}$ and $\mathbf{A}$ are the current density and vector potential, respectively. For the Pippard theory,

$$K(k) = \frac{6\pi\xi}{\xi_0\Lambda c^2}\frac{1}{\xi^3 k^3}[(1+\xi^2 k^2)\tan^{-1}\xi k - \xi k]\qquad (4)$$

where $\Lambda = 4\pi\lambda_L^2/c^2$. When the kernel of Eq. (4) is substituted into (2) the following result is obtained:

$$\left(\frac{\kappa}{\kappa_0}\right)_{\text{spec}} = 1 - 2\sum_{n=0}^{\infty}\left[\frac{\pi^2}{4}(2n+1)^2\right.$$

$$+\frac{1}{\beta\alpha^2(2n+1)^3}\{[1+\alpha^2(2n+1)^2]$$

$$\left.\times\arctan\alpha(2n+1) - \alpha(2n+1)\}\right]^{-1},\qquad (5)$$

where

$$\alpha = \frac{\pi}{2}\frac{\xi}{a}\quad\text{and}\quad\beta = \frac{\pi}{3}\frac{\xi_0\lambda_L^2}{a^3}.\qquad (6)$$

In general, the susceptibility as defined by Eq. (5) must be evaluated numerically. However, in the impure or London limit, a simple expression for κ/κ_0 can be derived. This limit is obtained when the coherence length is short enough so that any variation in vector potential occurs slowly over a coherence length, i.e., when $\xi k \to 0$. In this limit, the kernel of Eq. (4) becomes

$$K(k) \to 4\pi\xi/\xi_0\Lambda c^2,\qquad (7)$$

which gives a local relationship between the current and vector potential, because K is now a constant, independent of k. When Eq. (7) is substituted into (2), the series can be summed exactly to obtain

$$(\kappa/\kappa_0)_{\text{spec}} = 1 - (\xi_0\lambda_L^2/\xi a^2)^{1/2}\tanh(\xi a^2/\xi_0\lambda_L^2)^{1/2}.\qquad (8)$$

From Eq. (8), an interesting result can be obtained. The relationship between the weak-field susceptibility and the weak-field penetration depth, δ_0, is given by Ginzburg and Landau[5] to be

$$\kappa/\kappa_0 = 1 - (\delta_0/a)\tanh(a/\delta_0).\qquad (9)$$

Comparing Eqs. (8) and (9), it is clear that in the impure limit

$$\delta_0 = (\xi_0\lambda_L^2/\xi)^{1/2},\qquad (10)$$

which is the same result as that obtained by Pippard[2] for the bulk penetration depth in the impure limit.

[5] V. L. Ginzburg and L. D. Landau, Zh. Eksperim. i Teor. Fiz. **20**, 1064 (1950).
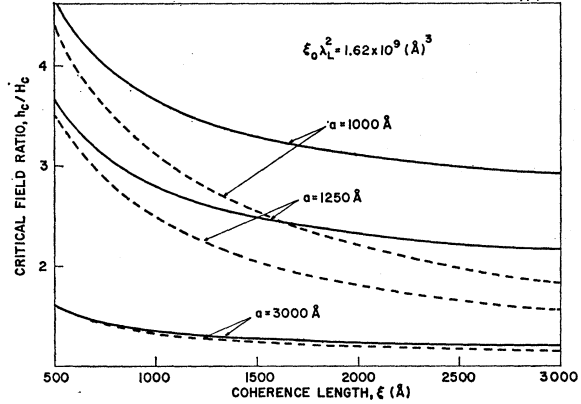

FIG. 1. The theoretical dependence of critical field upon coherence length. The curves shown are plots of the ratio of film critical field to bulk critical field vs coherence length and are calculated for various values of half-thickness a, holding $\xi_0\lambda_L^2$ constant and equal to 1.62×10^9 (Å)^3, a value previously found appropriate at 0.9 T_c for pure indium. The solid curves are the exact results of the model and are calculated from Eqs. (11) and (5). The dashed curves are approximate results valid in the impure limit and are calculated from Eqs. (11) and (8).

Having calculated κ/κ_0 from Eqs. (5) or (8), the film critical fields are calculated from κ/κ_0 using the theoretical relations derived by Ginzburg and Landau,[5] which are of the form

$$h_c/H_c = G(\kappa/\kappa_0),\qquad (11)$$

where G is a function which can be numerically evaluated, and is plotted in Fig. 2 of I. Mean free path effects upon the critical fields of thin films can be calculated in this model through the Pippard relation for the coherence length, which is

$$1/\xi = 1/\xi_0 + 1/\gamma l,\qquad (12)$$

where l is the intrinsic electronic mean free path in the normal state and γ is a constant, about one in value. Because the BCS theory, as modified by Mattis and Bardeen[6] to include mean free path effects, indicates that γ should be equal to one, we will henceforth set $\gamma = 1$ in Eq. (12).

In Fig. 1 are shown plots of the variation of film critical field with coherence length, ξ, for various film thicknesses. The solid curves are calculated from Eqs. (11) and (5). The dashed curves are calculated from Eq. (11) and the limiting expression of (8). All of the curves were calculated for $\xi_0\lambda_L^2 = 1.62\times10^9$ (Å)^3, a value found in I to be appropriate for indium at a reduced temperature of $t = 0.9$. Figure 1 indicates, as one might expect, that the critical field of a film increases for decreasing coherence length as well as decreasing thickness. In Fig. 2 are shown plots of h_c/H_c vs ξ for various values of $\xi_0\lambda_L^2$, but with $a = 1250$ Å, i.e., with a thickness of 2500 Å. The solid and dashed curves have the same significance as in Fig. 1. As Fig. 2

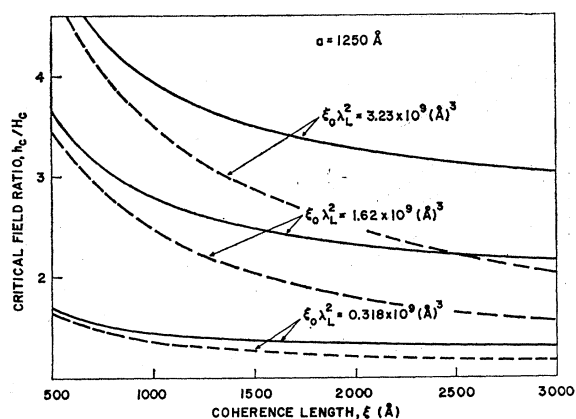[6] D. C. Mattis and J. Bardeen, Phys. Rev. **111**, 412 (1958).

FIG. 2. The theoretical dependence of critical field upon coherence length. The curves shown are plots of the ratio of film critical field to bulk critical field vs coherence length and are calculated for various values of $\xi_0\lambda_L{}^2$, holding the half-thickness a fixed at 1250 Å. The solid and dashed curves have the same significance as in Fig. 1.

indicates, h_c/H_c increases for increasing $\xi_0\lambda_L{}^2$ (i.e., increasing temperature) and decreasing ξ.

To compare the theoretical model of Eq. (1) to critical field data obtained for alloy films, one must know how ξ varies with the composition of the films. This information is obtained from Eq. (12) which relates ξ to the electronic mean free path in the normal state. Since the product of resistivity and mean free path is, for a given material, a constant, i.e.,

$$\rho l = A, \qquad (13)$$

the quantity ξ can be calculated from the resistivity of the alloy samples by means of the relation

$$1/\xi = 1/\xi_0 + \rho/A. \qquad (14)$$

However, when Eq. (14) is applied to thin films, the appropriate value of A will, in general, not be the same as that deduced for bulk specimens. For the sake of discussion, consider the simplest case, a metal having cubic symmetry. In a bulk specimen, the electrical conductivity is a scalar, and the constant A is inversely proportional to the area of the Fermi surface, excluding those regions touching a zone boundary.[7,8] In thin films, however, when surface scattering is important, electrons moving at different angles to the surface of the film contribute differently to the total current. For different orientations of the crystal axes relative to the surface, different groups of electrons become effective. Thus, the apparent dc conductivity (and hence the constant A) depends upon the orientation of the surface relative to the crystal axes.[9] When the orientation is such that a large number of electrons are traveling at small angles to the surface of the film., i.e., when that

part of the Fermi surface corresponding to such angles has a large radius of curvature, the apparent dc conductivity will be high and A will be small; when the effective part of the Fermi surface has a small radius of curvature, the apparent conductivity will be low and A will be large. In noncubic metals (indium is tetragonal), the situation is analogous but more complicated because the electrical condutivity, even in a bulk sample, is a second-order tensor. For films which are polycrystalline with randomly oriented crystallites, it is plausible that the nontensorial anisotropy effects due to surface scattering might average out to give the same value of A as in a polycrystalline bulk specimen. However, the indium films discussed in I and the indium alloy films to be discussed below, while not single crystals, do possess a very strong preferred orientation with the (101) planes of the body-centered tetragonal cell parallel to the substrate.[10] Hence, only a limited zone of the Fermi surface is effective in determining the dc conductivity.

Another effect which may be important in thin films has been suggested by Olsen.[11] To explain deviations from Matthiessen's law in thin indium wires, Olsen suggested that small angle scattering of electrons by phonons may give rise to a size dependent (and temperature dependent) resistivity. Theoretical calculations by Lüthi and Wyder[12] and Blatt and Satz[13] support this hypothesis. Such a mechanism might also cause A, as measured in thin films, to be different from values measured on bulk specimens because of differences in geometry.

Another point of importance concerns the quantity ξ. This quantity, like the quantities ξ_0 and λ_L, is a "bulk" parameter in the model presented in this paper. Hence, when ξ is calculated from Eq. (14), the appropriate value for ρ is not the measured film resistivity, for the latter includes boundary scattering.

3. EXPERIMENTAL

The indium-tin films reported on in this paper were evaporated from a single source onto fused quartz substrates and varied in composition from 0.02 to 4.6 at.% tin. Because of the relatively large difference in the evaporation rates of indium and tin, the tin content of films produced by this technique differed from that of the crucible melt. However, the compositions could be varied over the desired range of 0–5 at.% Sn by adjusting the melt compositions and the evaporation temperatures and times. The melt consisted of high-purity (99.999% pure Tadanac Brand) indium and tin inserted onto a previously degassed tantalum crucible. To avoid highly agglomerated films, the film substrates were maintained in contact with a reservoir held at liquid nitrogen temperature. Further details of the evaporation

[7] R. G. Chambers, Proc. Roy. Soc. (London) **A215**, 481 (1952).
[8] J. M. Ziman, Electrons and Phonons (Oxford University Press, New York, 1960), Chapter VII.
[9] R. Englman and E. H. Sondheimer, Proc. Phys. Soc. (London) **B69**, 449 (1956).

[10] M. G. Miksic (to be published).
[11] J. L. Olsen, Helv. Phys. Acta **31**, 713 (1958).
[12] B. Lüthi and P. Wyder, Helv. Phys. Acta **33**, 667 (1960).
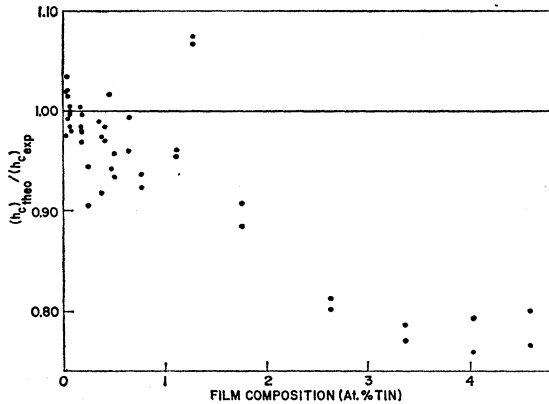[13] F. J. Blatt and H. G. Satz, Helv. Phys. Acta **33**, 1007 (1960).

FIG. 3. Comparison of the theoretical model to the experimental data. The points shown are the calculated ratios of theoretically predicted film critical field to experimentally observed critical field at 0.9 T_c, plotted as a function of film composition. The theoretical critical fields were calculated for each film from Eqs. (11) and (5) using the measured values of thickness; with $\xi_0\lambda_L^2 = 1.62 \times 10^9 (\text{Å})^3$; and with $\xi = \xi_0 = 2600$ Å (i.e., mean free path effects are neglected).

techniques and the film properties other than critical field will be discussed in a future publication.

The compositions of the films were determined by Miksic[10] using an x-ray fluorescence technique capable of determining the tin content of these films to ±0.05 at.% Sn.

The methods for measuring the film thicknesses and critical magnetic fields have been discussed previously[14] and will not be repeated here.

4. COMPARISON OF EXPERIMENTAL DATA TO THEORETICAL MODEL

As Sec. 2 of this paper indicates, in order to calculate the critical field ratio h_c/H_c for a superconducting film, one must know the film thickness and the nonlocal parameters ξ and $\xi_0\lambda_L^2$. The quantity ξ has been calculated for each film from Eq. (14) using the intrinsic resistivity, i.e., the resistivity which would have been obtained if boundary scattering were not present. The latter was calculated from the measured resistivity and thickness by means of Fuchs' relation.[15] It is felt that this procedure is justified in these dilute alloys since Fuchs' model has been shown to be in reasonably good agreement with resistivity measurements made upon evaporated indium films,[14] thin indium foils,[16] and fine indium wires.[11] The values for the constant A of Eqs. (13) and (14) obtained from these experiments are 2.0×10^{-11} Ω-cm^2, 1.6×10^{-11} Ω-cm^2, and 1.8×10^{-11} Ω-cm^2, respectively. It is interesting to note that these values for A are in reasonable agreement with one another yet differ considerably from the "bulk" values of 0.89×10^{-11} Ω-cm^2 obtained by Roberts,[17] and 0.57×10^{-11} Ω-cm^2

[14] A. M. Toxen, Phys. Rev. 123, 442 (1961).
[15] K. Fuchs, Proc. Cambridge Phil. Soc. 34, 100 (1938).
[16] A. Gaide and P. Wyder (to be published).
[17] D. C. Roberts (unpublished). See T. E. Faber, Proc. Roy. Soc. (London) A241, 531 (1957).

by Dheer.[18] Values for the quantity A can be obtained, not only from dc resistivity measurements on thin specimens and high-frequency anomalous skin effect measurements on bulk samples, but also from critical field measurements on thin films. It is shown in I that A, on the basis of a simple free-electron model, is related to $\xi_0\lambda_L^2$, which in turn can be obtained from critical field measurements. On the basis of the specular reflection model, one obtains $A = 0.98 \times 10^{-11}$ Ω-cm^2. For the diffuse scattering model, one obtains $A = 0.74 \times 10^{-11}$ Ω-cm^2. Whether these two values are "thin film" or "bulk" values is, perhaps, debatable. However, it is felt that, because ξ_0 and λ_L are bulk, parameters, these values for A are bulk quantities, i.e., they are characteristic of the entire Fermi surface, not just a limited area of the Fermi surface which might be important in determining the conductivity of thin films. At any rate, it is clear that the experimental values for A fall into two groups: $0.6-0.98 \times 10^{-11}$ Ω-cm^2 for the "bulk" values, and $1.6-2.0 \times 10^{-11}$ Ω-cm^2 for the "thin film" values.

In Figs. 3, 4, and 5 are shown plots of the ratio of the theoretically predicted h_c to the experimentally observed h_c at 0.9 T_c. What is actually calculated from the theoretical model of Sec. 2 is the ratio of the film critical field to the bulk critical field. To calculate the film critical field, one must know the bulk critical field as a function of temperature and composition. This information was obtained from as yet unpublished data of D. J. Quinn on specimens of indium containing up to 6 at.% tin. In Fig. 3 we have taken $\xi = \xi_0$ for all of the films, i.e., we have neglected mean free path effects in calculating the theoretical film critical field, $(h_c)_\text{theo}$. In
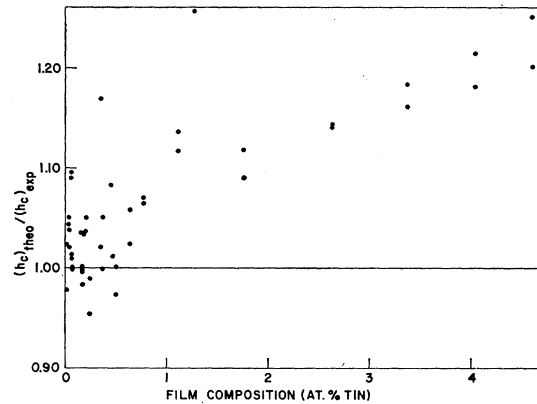

FIG. 4. Comparison of the theoretical model to the experimental data. The points shown are the calculated ratios of theoretically predicted film critical field to experimentally observed critical field at 0.9 T_c, plotted as a function of film composition. The theoretical critical fields were calculated for each film from Eqs. (11) and (5) using the measured values of thickness; with $\xi_0\lambda_L^2 = 1.62 \times 10^9 (\text{Å})^3$; and with ξ calculated from Eq. (12) for $\xi_0 = 2600$ Å, $\gamma = 1$, and l determined from the measured thicknesses and resistivities by means of Fuchs' model for $\rho l = 0.98 \times 10^{-11}$ Ω-cm^2.

[18] P. N. Dheer, Proc. Roy. Soc. (London) A260, 333 (1961).

Fig. 4 we have calculated ξ for each film on the assumption that $A = 0.98 \times 10^{-11}$ Ω-cm^2, and in Fig. 5 we have taken $A = 2.0 \times 10^{-11}$ Ω-cm^2. In each of the plots we have taken $\xi_0 \lambda_L^2 = 1.62 \times 10^9$ (Å)^3 and $\xi_0 = 2600$ Å, the values found in I to be appropriate for indium at 0.9 T_c. We have also assumed that $\xi_0 \lambda_L^2$, ξ_0, and A are independent of composition over the composition range shown, 0–4.6 at.% Sn.

In Fig. 3, where we have neglected mean free path effects, we see that the theoretical values of h_c are too small, the ratio $(h_c)_{\text{theo}}/(h_c)_{\text{exp}}$ varying systematically from about one at 0 at.% Sn to 0.78 at 4.6 at.% Sn. In Fig. 4, where we have taken $A = 0.98 \times 10^{-11}$ Ω-cm^2, the values of $(h_c)_{\text{theo}}$ are too large, the ratio $(h_c)_{\text{theo}}/(h_c)_{\text{exp}}$ becoming about 1.22 at 4.6 at.% Sn. Had we taken $A = 0.57 \times 10^{-11}$ Ω-cm^2, the disagreement would have been even worse. In Fig. 5, where we have taken $A = 2.0 \times 10^{-11}$ Ω-cm^2, the agreement between $(h_c)_{\text{theo}}$ and $(h_c)_{\text{exp}}$ is reasonably good. For most of the films, $(h_c)_{\text{theo}}$ and $(h_c)_{\text{exp}}$ agree within $\pm 6\%$. If we assume that A varies slightly with composition, decreasing from 2.0×10^{-11} Ω-cm^2 at 0 at.% Sn to 1.6×10^{-11} Ω-cm^2 at 3 at.% Sn, then increasing to 1.8×10^{-11} Ω-cm^2 at 5 at.% Sn, we can get exact agreement within the scatter of the data, between $(h_c)_{\text{theo}}$ and $(h_c)_{\text{exp}}$. However, the data may not be accurate enough to justify such detailed examination.

In Fig. 6 are shown the values of coherence length calculated for each film with $A = 2.0 \times 10^{-11}$ Ω-cm^2 and $\xi_0 = 2600$ Å, and plotted as a function of film composition. Although there is a fair amount of scatter, one can see that the data lie on a smooth curve. To see how one might expect the critical fields of thin alloy films to vary with composition at constant thickness, we have plotted, in Fig. 7, the quantity h_c/H_c versus film composition. We have taken the dependence of ξ upon composition to be given by the solid curve of Fig. 6, and
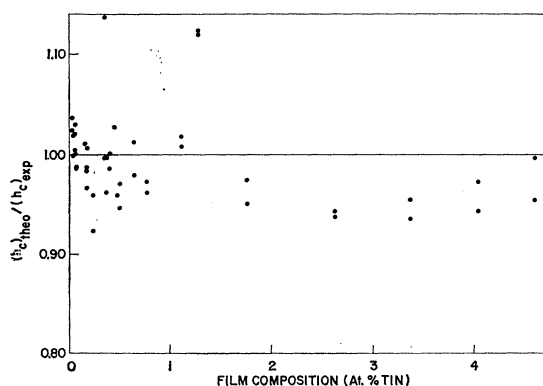

FIG. 5. Comparison of the theoretical model to the experimental data. The points shown are the calculated ratios of theoretically predicted film critical field to experimentally observed critical field at 0.9 T_c. The theoretical critical fields were calculated for each film in the same manner as in Fig. 4, except that ρl was assumed to be 2.0×10^{-11} Ω-cm^2.
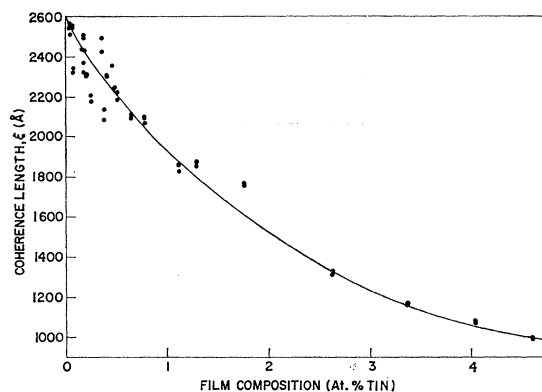

FIG. 6. Variation of coherence length with composition. The values of coherence length shown were calculated for each film from Eq. (12) with $\xi_0 = 2600$ Å, $\gamma = 1$, and l determined from the measured thicknesses and resistivities by means of Fuchs' model, under the assumption that $\rho l = 2.0 \times 10^{-11}$ Ω-cm^2 (the value that gives the best agreement between theory and experiment).

have calculated h_c/H_c from Eqs. (5) and (11) with $\xi_0 \lambda_L^2 = 1.62 \times 10^9$ (Å)^3. (See also Fig. 1.)

There are several significant points to be made. First, there is the fact that the observed variation of critical field with composition and thickness is in good agreement with the theoretical model. Second, it is important that the value for A, which must be used to get this good agreement, is the "thin film" value 1.6–2.0×10^{-11} Ω-cm^2 obtained from resistivity measurements on thin specimens rather than the bulk value of 0.6–0.98×10^{-11} Ω-cm^2 obtained from high frequency or critical field measurements. Third, one can obtain a detailed fit of the theoretical model to the experimental data over the entire range of composition 0–5 at.% Sn by postulating a variation in A of no more than 20%. In view of the fact that indium has a complex Fermi surface which extends into the third Brillouin zone,[19] this would not be an unreasonable assumption. Fourth, the values of $\xi_0 \lambda_L^2$ and ξ_0 obtained previously from measurements on pure indium films seem to fit the data of the dilute alloy films.

There are three main sources of experimental error. First, there is the uncertainty in the composition which is estimated to be ± 0.05 at.% Sn. A second source of error is related to the fact that the background pressure in the vacuum system during an evaporation would occasionally rise suddenly, perhaps due to insufficient preoutgassing of the melt, crucible, etc. This would result in films of lower purity which would have critical fields higher than one would expect from their tin content. The third source of error is in the film thicknesses, which are calculated from measurements of film resistance. In addition to random errors in measurement, there may occur occasional systematic errors resulting from agglomeration in the films. When the thermal contact between substrate and liquid nitrogen reservoir is poor, as sometimes happens, the substrate will be too
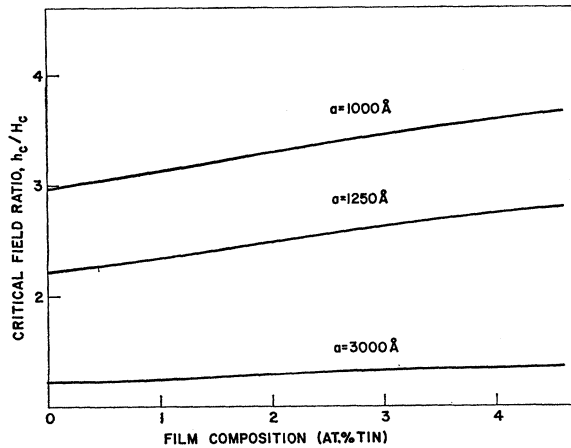
[19] J. A. Rayne, Phys. Rev. 129, 652 (1963).

FIG. 7. The theoretical dependence of critical field upon composition. The curves shown are plots of the ratio of film critical field to bulk critical field vs film composition and are calculated from Eqs. (11) and (5) for various values of half-thickness a, holding $\xi_0\lambda_L^2$ constant and equal to 1.62×10^9 $(\text{Å})^3$. The variation of ξ with composition was taken to be that of the smooth curve of Fig. 6.

warm and agglomeration will occur. This will result in a film having a resistance higher than that of a comparable unagglomerated film. Thus, the thickness calculated for this film will be too small or, looked at another way, the measured critical field will be lower than that expected from the thickness measurement. Hence, the measured critical fields can be either too large or too small. All of these sources of error are likely to be more serious for the most dilute films and Figs. 3–6 bear out this conclusion.

5. ARE SIZE EFFECTS EQUIVALENT TO MEAN FREE PATH EFFECTS?

It was suggested by Abrikosov and Gor'kov[20] that expressions derived for the penetration depth and complex impedance of superconducting alloys were also applicable to films of a pure substance thinner than a penetration depth. Their reasoning was that, in a polycrystalline thin film, scattering at crystallite boundaries will limit the electronic mean free path and, hence, the coherence length to less than the penetration depth. Under these conditions, a local relationship between the current density and vector potential known as the London limit will be applicable. Calculations of the type suggested by Abrikosov and Gor'kov have been carried out by Douglass[21] starting from an extension of the Ginzburg-Landau theory by Gor'kov[22] which takes into account mean free path effects.

Whether size effects can be described by a mean free path characterizing boundary scattering will depend, first of all, on what type of boundary conditions are

appropriate. If the electrons undergo specular reflection at the film surface, there will not be any size dependence of mean free path. Since the size of an electron "pair" in the superconducting state is of the order of the coherence length, which is typically several thousand angstroms, it is not inconceivable that an appreciable fraction of the pairs could undergo specular reflection at film surfaces. On the other hand, if the electrons undergo diffuse scattering at film boundaries, one might be able to describe size effects in terms of the mean free path for boundary scattering.

In films which are thin compared to the coherence length, ξ, however, the magnetic field is limited to a region small compared to ξ, and so it is the Pippard limit, rather than the London limit, which applies.[23] One can see this immediately by examining the Pippard kernel given in Eq. (4). The London limit is obtained when the coherence length is short enough so that any variation in field occurs slowly over a coherence length, i.e., when $\xi k \to 0$. In this limit, we obtained Eq. (7). In the thin film, however, the important Fourier components of the vector potential will be those for which k is of the order of $1/a$. The quantity ξ, which is a bulk parameter, is independent of thickness. Hence, for $a \to 0$, the correct limit of $K(k)$ is that for $\xi k \to \infty$. In this limit, which is just the opposite of the London limit, we obtain from Eq. (4)

$$K(k) \to 3\pi^2/\xi_0\Lambda c^2 k, \qquad (15)$$

a result quite different from Eq. (7). Since $K(k)$ as given by Eq. (15) is now a function of k, it will lead to a nonlocal relationship between the current and vector potential.

It is quite interesting, though, that one can get a result quite similar to the "correct" limiting expression for the critical fields of very thin films by a dubious, if not incorrect, derivation. In this paper thus far, in I, and in Schrieffer's paper,[4] it has been assumed that a film is a thin slab of "bulk" material having the coherence length and London penetration depth of a similar bulk sample, i.e., in the calculations of current distribution, the finite thickness enters purely through the boundary conditions. It is conceivable that one might take an alternative point of view, that the film is an infinite specimen with a distribution of scattering centers so situated as to give the proper boundary scattering. In the latter case, the film "thickness" is reflected in the distribution of scattering centers and hence has a direct influence on the coherence length through the mean free path. This approach has an immediate difficulty; it is explicitly assumed by Mattis and Bardeen[6] in their derivation of the kernel in the presence of scatterers, that the scatterers are randomly distributed with resultant phase cancellations. This assumption was also made by Gor'kov[22] and it seems to be

[20] A. A. Abrikosov and L. P. Gor'kov, Zh. Eksperim. i Teor. Fiz. 35, 1558 (1958) [translation: Soviet Phys.—JETP 8, 1090 (1959)].
[21] D. H. Douglass, Jr., Phys. Rev. 124, 735 (1961).
[22] L. P. Gor'kov, Zh. Eksperim. i Teor. Fiz. 37, 1407 (1959) [translation: Soviet Phys.—JETP 10, 998 (1960)].

[23] J. Bardeen and J. R. Schrieffer, in Progress in Low Temperature Physics, edited by C. J. Gorter (Interscience Publishers, Inc., New York, 1960), Vol. III, p. 233.

implicit in the Pippard model. However, to obtain boundary scattering, the distribution of scatterers is quite "nonrandom." Let us ignore this difficulty and proceed. Assume that the formulas derived for the London or impure limit are applicable to thin films. If we substitute the expression for the penetration depth given by Eq. (10) into (5) of I, which gives the critical field of a thin film to be

$$h_c/H_c = 6^{1/2}\delta_0/a,   (16)$$

we get

$$h_c/H_c = (6\xi_0\lambda_L^2/\xi a^2)^{1/2}.   (17)$$

If we now set the coherence length equal to the film thickness, $2a$, we get

$$h_c/H_c = \sqrt{3}(\xi_0\lambda_L^2/a^3)^{1/2},   (18)$$

a result differing from Eq. (15) of I by only a numerical constant, $\sqrt{3}$ instead of 2.01. Although this derivation yields the correct dependence of critical field upon thickness, it involves the arbitrary assumptions that the London limit is applicable to thin films and that $\xi = 2a$. But if $\xi = 2a$, then ξk is of order one and the London limit is not applicable. Indeed, considering the thin film to be a bulk superconductor with short mean free path, it would seem more natural to set the coherence length equal to the mean free path. The theoretical model by Fuchs gives the relation between the mean free path l and thickness $2a$ to be

$$l \simeq 1.5a \ln(0.76l_0/a)   (19)$$

in the thin-film limit, where l_0 is the intrinsic mean free path. If Eq. (19) is substituted for ξ into (17), the result is

$$h_c/H_c = 2[\xi_0\lambda_L^2/a^3 \ln(0.76l_0/a)]^{1/2},   (20)$$

which differs from Eq. (15) of I by the logarithmic term. The origin of the logarithmic term was the assumption that $\xi k \rightarrow 0$, which is the condition under which Eq. (17) is valid. It is clear that if the coherence length is given by Eq. (19), and if k is of order $1/a$, then $\xi k \rightarrow \infty$ for $a \rightarrow 0$, and it is not legitimate to use (17).

One can derive in a different manner an expression similar to Eq. (20), which shows clearly that the logarithmic term results from neglecting the variation in the vector potential in a thin film. The Pippard relation between the current and vector potential is

$$\mathbf{j}(\mathbf{r}) = -\frac{3}{4\pi c\Lambda\xi_0} \int \frac{\mathbf{R}[\mathbf{R}\cdot\mathbf{A}(\mathbf{r}')]}{R^4} e^{-R/\xi} d\mathbf{r}',   (21)$$

where $\mathbf{R} = \mathbf{r} - \mathbf{r}'$ and div $\mathbf{A} = 0$. Consider a slab of thickness $2a$ bounded by two infinite planes. If we assume that we can neglect the variation in the vector potential over a coherence length and hence replace $\mathbf{A}(\mathbf{r}')$ by

$\mathbf{A}(\mathbf{r})$, then $\mathbf{A}(\mathbf{r})$ can be removed from under the integral sign and the integration can be carried out to give the result[24]

$$\mathbf{j}(\mathbf{r}) = -\frac{3a}{\Lambda c\xi_0}\left\{ -\mathrm{Ei}\left(-\frac{\alpha}{2}\right)\left[\frac{1}{2} - \frac{\alpha^2}{48}\right] + \frac{2}{3\alpha}(1 - e^{-\alpha/2}) \right. $$
$$\left. -\frac{e^{-\alpha/2}}{12}\left(1 - \frac{\alpha}{2}\right) \right\}\mathbf{A}(\mathbf{r}),   (22)$$

where $\alpha = 2a/\xi$ and $\mathrm{Ei}(X)$ is the exponential integral.[25] In the impure limit, $\alpha \rightarrow \infty$, Eq. (22) gives

$$\mathbf{j}(\mathbf{r}) = -\frac{\xi}{\xi_0\Lambda c}\mathbf{A}(\mathbf{r}).   (23)$$

By comparing Eq. (23) to (3), we obtain the kernel, $K(k)$, to be the same as that given by (7), as it should be. In the thin-film limit, $\alpha \rightarrow 0$, Eq. (22) becomes

$$\mathbf{j}(\mathbf{r}) = -\frac{3a}{2\Lambda c\xi_0} \ln\frac{\xi}{a}\mathbf{A}(\mathbf{r}),   (24)$$

giving for the kernel

$$K(k) = \frac{6\pi a}{\Lambda c^2\xi_0} \ln\frac{\xi}{a},   (25)$$

a result quite different from the correct relation of Eq. (15). From Eqs. (21), (19), and (16), we find the critical field calculated from (25) to be

$$h_c/H_c = 2[\xi_0\lambda_L^2/a^3 \ln(\xi/a)]^{1/2},   (26)$$

a result virtually identical to Eq. (20), differing only in the replacement of $0.76l_0$ by ξ. It is important to note that in deriving Eq. (26) it was not necessary to use any theoretical model for the thickness dependence of boundary scattering, e.g., Fuchs' model. The logarithmic term in Eq. (26) was a direct consequence of the assumption that $\mathbf{A}(\mathbf{r}')$ was slowly varying over a coherence length and could be replaced by $\mathbf{A}(\mathbf{r})$.

Thus, we conclude that size effects are not equivalent to mean free path effects, or put another way, boundary scattering is not equivalent to scattering by defects distributed randomly throughout the volume of the superconductor. As we have shown, in the limit of a high concentration of randomly distributed defects, the London or local limit obtains; in the thin limit, where boundary scattering predominates, the Pippard or nonlocal limit obtains. Hence, to describe the superconducting properties of films, we must "sort out" the effects of randomly distributed scatterers from thickness

[24] R. R. Haering (private communication).
[25] E. Jahnke and F. Emde, *Tables of Functions* (Dover Publications, New York, 1945), p. 1.
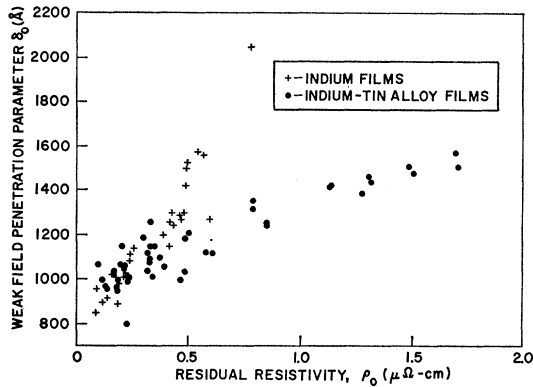
FIG. 8. Comparison of weak field penetration depths of pure indium films to those of the indium-tin alloy films. The penetration depths are calculated from the measured critical fields by means of the Ginzburg-Landau theory and are plotted vs the directly measured residual resistivities. In the thin indium films, the resistivity is largely due to boundary scattering; in the alloy films, it is caused by a combination of boundary scattering and impurity scattering.

effects. The experimental evidence appears to substantiate this conclusion.

In Fig. 8 are plotted values of the weak-field penetration depth, δ_0, versus measured residual resistivity, for pure indium films and indium-tin alloy films. These values of δ_0 were calculated from the critical field data at $0.9\ T_c$ using the Ginzburg-Landau theory. (See Fig. 1 of I.) If the ρl constant were the same for the pure and alloy films, one would expect the two sets of data to coincide in the high-resistivity limit in the event that boundary scattering and random defect scattering were equivalent. As Fig. 8 indicates, the two sets of data diverge in the high-resistivity limit. To account for this divergence, one would have to postulate a 300% change in the constant A over the range 0–5 at.% Sn. This seems too large to be reasonable. On the other hand, we have seen in I and in Sec. 4 of this paper that the proposed theoretical model, which treats thickness effects and mean free path effects independently, fits the critical field data of the pure indium and the alloy films reasonably well if we assume a constant value for A. We can even force a fit of the theoretical model to the critical field data by assuming a variation in A of only 20% over the range 0–4.6 at.% Sn.

6. SUMMARY OF CONCLUSIONS

The contents of this paper can be divided into two broad categories. The first part of the paper, Secs. 2–4, contains a discussion of mean free path and thickness effects upon the critical fields of thin films. Theoretical results, calculated from the model proposed in a previous paper[1] and using the Pippard kernel with specular boundary conditions, are compared to experimental data obtained for alloy films of indium containing 0–4.6 at.% Sn. In making the comparison, the values of $\xi_0\lambda_L^2$ and ξ_0 were taken to be those previously determined by fitting the theoretical model to critical field data on pure indium films. The coherence length, ξ, was calculated from the intrinsic mean free path which in turn was calculated for each film from the measured residual resistivity and thickness for three values of the ρl constant: infinity, which leads to the result $\xi = \xi_0$, i.e., which neglects mean free path effects; 0.98×10^{-11} Ω-cm^2, a value obtained from critical field measurements on indium films; and 2.0×10^{-11} Ω-cm^2, a value obtained from resistivity measurements on thin indium films. Of the three values for ρl, the best agreement between theory and experiment was obtained for 2.0×10^{-11} Ω-cm^2. For this value of ρl the difference between the measured and calculated film critical fields was less than $\pm 6\%$ for most of the films measured. If we postulate a 20% variation in ρl over the composition range 0–4.6 at.% Sn, we obtain exact agreement within experimental error between theory and experiment.

The second portion of the paper, Sec. 5, contains a discussion of whether boundary scattering is equivalent to scattering by randomly distributed defects in films. It is concluded that the two are not equivalent. In fact, it is demonstrated that whereas the London or "local" limit obtains in the presence of high concentrations of randomly distributed defects, the Pippard or nonlocal limit obtains in very thin films.

ACKNOWLEDGMENTS